analytical chemistry

Article

pubs.acs.org/ac

Carbon-Dot-Based Ratiometric Fluorescent Probe for Imaging and Biosensing of Superoxide Anion in Live Cells

Xiang Gao,[†] Changqin Ding,[†] Anwei Zhu,[‡] and Yang Tian*[,‡]

[†]Department of Chemistry, Tongji University, Siping Road 1239, Shanghai 200092, P. R. China

[‡]Department of Chemistry, East China Normal University, North Zhongshan Road 3663, Shanghai 200062, P. R. China

Supporting Information

ABSTRACT: In this article, a ratiometric fluorescent biosensor for $O_2^{\bullet-}$ was developed, by employing carbon dots (C-Dots) as the reference fluorophore and hydroethidine (HE), a specific organic molecule toward $O_2^{\bullet-}$, playing the role as both specific recognition element and response signal. The hybrid fluorescent probe CD-HE only emitted at 525 nm is ascribed to C-Dots, while HE was almost nonfluorescent, upon excitation at 488 nm. However, after reaction with $O_2^{\bullet-}$, a new emission peak ascribed to the reaction products of HE and $O_2^{\bullet-}$ was clearly observed at 610 nm. Meanwhile, this peak gradually increased with the increasing concentration of $O_2^{\bullet-}$ but the emission peak at 525 nm stayed constant, leading to a ratiometric detection of $O_2^{\bullet-}$. The inorganic−organic fluorescent sensor exhibited high sensitivity, a broad dynamic linear range of $\sim 5 \times 10^{-7}$−1.4×10^{-4} M, and low detection limit down to 100 nM. The present probe also showed high accuracy and excellent selectivity for $O_2^{\bullet-}$ over other reactive oxygen species (ROS), metal ions, and so on. Moreover, the C-Dot-based inorganic−organic probe demonstrated long-term stability against pH changes and continuous light illumination, good cell-permeability, and low cytotoxicity. Accordingly, the developed fluorescent biosensor was eventually applied for intracellular bioimaging and biosensing of $O_2^{\bullet-}$ changes upon oxidative stress.

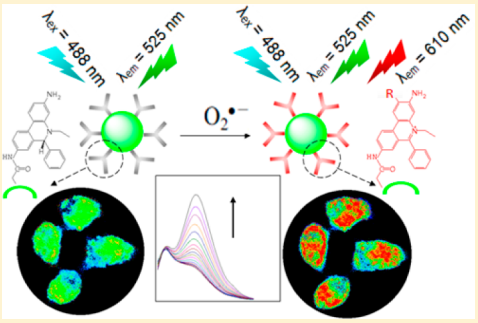

Reactive oxygen species (ROS) are a class of radical and nonradical oxygen-containing molecules that show high reactivity with lipids, proteins, and nucleic acids. ROS are considered as the mediators of biochemistry of cellular pathology and constitute the so-called oxidative stress in unwanted excess, which may be a major contributing factor for diseases such as diabetes, cancer, and molecular neurodegenerative disorders including Alzheimer's and Parkinson's diseases.[1,2] Superoxide ($O_2^{\bullet-}$), a product of one-electron reduction of molecular oxygen, is the "primary" species of ROS. On one hand, it serves as a precursor of other ROS, such as hydrogen peroxide (H_2O_2), hydroxyl radical ($^{\bullet}OH$), and so on. On the other hand, it can inactivate nitric oxide (NO), thereby causing endothelial dysfunction.[3] Depending on concentration, location, and context, $O_2^{\bullet-}$ and other ROS can be either "friends" or "foes". At low concentrations, $O_2^{\bullet-}$ plays an important role as a regulatory mediator in signaling processes. Excessive accumulation of $O_2^{\bullet-}$ may cause damage to biological membranes, tissues, and organisms.[4,5] Thus, it is of great significance to design and develop the analytical strategies for determination the concentration of $O_2^{\bullet-}$ with high selectivity and accuracy in live cells, tissues, and organisms.

Over the past couple of decades, considerable attention has been paid on the development of analytical methods for $O_2^{\bullet-}$ detection because the elucidation of biological functions of $O_2^{\bullet-}$ has become an important research area. Many elegant techniques have been reported such as electron spin resonance (ESR) spectroscopy, electrochemical determination, chromatography, chemluminescence, and fluorescence spectroscopy.[6−10] Our group is very interested in development of analytical methods for ROS determination and have established several reliable and durable electrochemical and fluorescent approaches for monitoring of $O_2^{\bullet-}$ and other ROS in live cells and animals.[11−15] Compared with other techniques, the fluorescence probes exhibit more advantages including high sensitivity and selectivity and direct monitoring in live cells, tissues, and animals.[16−19] Many elegant "turn-on" fluorescent sensors have been designed for determination of intracellular $O_2^{\bullet-}$.[20−23] However, to the best of our knowledge, few papers have been reported on the development of ratiometric fluorescence sensors for determination of $O_2^{\bullet-}$ in live cells because it is still a challenging work to design and synthesize the dual-emission organic fluorophores which can be specific and sensitive to $O_2^{\bullet-}$. As a matter of fact, the ratiometric fluorescence measurements not only can improve the sensitivity of the detection but also can avoid interferences from background fluorescence. The reason is that the ratio of the fluorescent intensities at two wavelengths is independent of the probe concentration and the inhomogeneous distribution, the fluctuation of light-source intensity, and the sensitivity of instruments.[24−27]

Received: April 24, 2014
Accepted: June 16, 2014
Published: June 16, 2014

   dx.doi.org/10.1021/ac501499y | Anal. Chem. 2014, 86, 7071−7078

In this work, as shown in Scheme 1, carbon dots (C-Dots) were first conjugated with organic dye hydroethidine (HE), a

Scheme 1. Working Principle of Ratiometric Fluorescent CD-HE biosensor for $O_2^{\bullet-}$

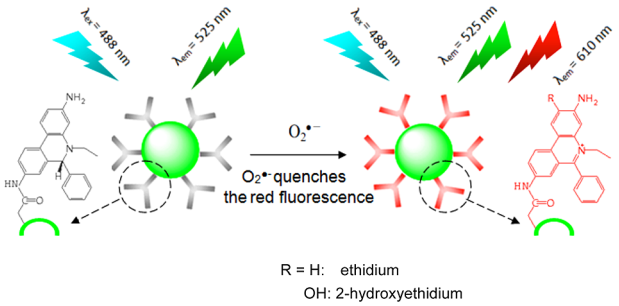

specific molecule toward $O_2^{\bullet-}$, to form an inorganic−organic ratiometric fluorescent sensor for $O_2^{\bullet-}$ detection with high selectivity and accuracy. Photoluminescent C-Dots have attracted growing interest because of their great potential in biological labeling, bioimaging, drug delivery, and optoelectronic device applications.[28−31] The C-dots combine several favorable attributes of traditional semiconductor-based quantum dots with higher quantum yields such as size- and wavelength-dependent luminescence emission, resistance to photobleaching, and ease of bioconjugation. More interestingly, compared to the semiconductor quantum dots, they have no burden of intrinsic toxicity or elemental scarcity and have no need for stringent, intricate, tedious, costly, or inefficient preparation steps. Thus, C-Dots are more fascinating and potentially useful for bioimaging and biosensing in live cells. Here, the electrochemically prepared C-Dots were used as the reference signal element, and hybridized with HE to form the ratiometric fluorescence probe CD-HE. In the inorganic−organic probe, HE played the role as specific recognition element for $O_2^{\bullet-}$, meanwhile as a response signal since almost nonfluorescent HE can react with $O_2^{\bullet-}$ with high selectivity to generate the products which showed an emission peak at 610 nm at an excitation wavelength of 488 nm.[32−38] Furthermore, the fluorescence emission peak observed at 610 nm gradually increased with the continuous addition of $O_2^{\bullet-}$, while the fluorescence emission at 525 nm ascribed to C-Dots had no obvious changes, leading to the ratiometric detection of $O_2^{\bullet-}$. The present ratiometric probe displayed high selectivity for $O_2^{\bullet-}$ detection over other ROS, metal ions, and so on, due to the specific recognition of HE toward $O_2^{\bullet-}$. Meanwhile, the CD-HE exhibited a good linearity with the concentration of $O_2^{\bullet-}$ from 500 nM to 30 μM and the detection limit was achieved to 100 nM. Compared with previous fluorescent probes for $O_2^{\bullet-}$,[39,40] the developed inorganic−organic ratiometric probe showed high accuracy and long-term stability and was consequently applied for intracellular bioimaging and ratiometric monitoring of $O_2^{\bullet-}$.

EXPERIMENTAL SECTION

Chemicals and Materials. Hydroethidine (HE), 1-ethyl-3-(3-(dimethylamino)propyl)carbodiimide (EDC), *N*-hydroxysuccinimide (NHS), potassium superoxide (KO_2), glutathione (GSH), dimethyl sulfoxide (DMSO), methyl thiazolyl tetrazolium (MTT), and lipopolysaccharides (LPS) from *Escherichia coli* were supplied by Sigma-Aldrich. Albumin from bovine serum (BSA), 2,2′-azobis (2-methylpropionamidine) dihydrochloride (AAPH), KH_2PO_4, $K_2HPO_4{\cdot}3H_2O$, NaOH, KCl, NaCl, $CuCl_2{\cdot}2H_2O$, $CaCl_2$, $FeCl_3$, $NiCl_2{\cdot}6H_2O$, $MnCl_2{\cdot}4H_2O$, $ZnCl_2$, $CoCl_2{\cdot}6H_2O$, $MgCl_2{\cdot}6H_2O$, and glucose were obtained from Sinopharm Chemical Reagent Co. Ltd. Hydrogen peroxide (H_2O_2, 30%), $NaNO_2$, NaClO, and $FeCl_2{\cdot}4H_2O$ were purchased from Aladdin Chemistry Co. Ltd. The dialysis tube (MWCO, 3500) was supplied by Ebioeasy Corporation.

The chemical generation of $O_2^{\bullet-}$ was performed by dissolving KO_2 in DMSO solution.[41] The concentration of $O_2^{\bullet-}$ was determined by recording the reduction of ferricytochrome c spectrophotometrically using an Agilent 8453 UV−vis-NIR spectrophotometer (Agilent Instruments) and using the extinction coefficient (21.1 mM^{-1} cm^{-1}) of ferrocytochrome c at 550 nm.[42] For the experiments of selectivity and competition test, hydroxyl radical ($^{\bullet}OH$) was produced by Fenton reaction (Fe^{2+}/H_2O_2 = 1:6). Peroxynitrite ($ONOO^-$) was chemically provided by H_2O_2 and $NaNO_2$. Hypochlorite ion (ClO^-) was generated by 150 μM NaClO. Nitric oxide (NO) and nitroxyl (HNO) were obtained from the solution of *S*-nitroso-*N*-acetyl-DL-penicillamine and Angeli's salt ($N_2Na_3O_3^+$), respectively. Alkyl peroxyl radical ($ROO^{\bullet}$) was obtained by thermolysis of AAPH in air-saturated solution at 310 K. The first singlet oxygen ($^1O_2$) was produced by H_2O_2 with NaClO.

Synthesis of C-Dots and CD-HE Probe. The C-Dots were synthesized by the reported electrochemical method. Briefly, electrolyte was prepared by adding 0.6 g of NaOH into 200 mL of ethanol and H_2O (199:1, v:v). Graphite rods (Sigma-Aldrich) were used as both anode and cathode electrodes. C-Dots were obtained in the prepared electrolyte under vigorous stirring for 16 h, with a current intensity of 20 mA cm^{-2}. Next, $MgSO_4$ (10 g, 5−7 wt %) was added to the C-Dots solution as a desiccant, stirred for 30 min. Afterward, the solution was stored for 24 h and followed by filtering to get rid of the salts. Finally, ethanol was removed by vacuum distillation. For preparation of the fluorescent probe for $O_2^{\bullet-}$, HE was conjugated with C-Dots by using EDC and NHS and denoted as CD-HE hereafter. Typically, 24 mg of EDC and 48 mg of NHS were added to 25 mg of C-Dots dissolved in 5 mL of PBS buffer (pH = 7.4). After stirred for 30 min, 1 mg of HE was added to the mixture and then stirred vigorously for 2 h. The nanohybrids were finally separated from free EDC/NHS and unreacted HE by three cycles of concentration/dilution (10:1), using a Nanosep centrifugal device (Pall Corporation, MW cutoff of 3 kDa) and redispersed in PBS buffer (pH = 7.4). The obtained solution was under filtration and stored at 4 °C for further use.

Instrumentation. Atomic force microscopy (Picoscan 2100 MI) and transmission electron microscopy (JEOL 2100) were employed to observe the morphology of C-Dots. The surface of C-Dots and the conjugation of HE and C-Dots were characterized by a Fourier transform infrared spectroscopy (Nicolet 6700, Thermo Electron). UV−vis spectroscopy (Agilent 8453) was employed for the measurements of optical absorption spectra. The fluorescence spectra were measured by a fluorescence spectroscopy (F-2700FL, Hitachi). Confocal images were observed using a confocal laser scanning microscope (Fluoview 1000, Olympus).

Cell Culture and MTT Assay. Cell culture media were obtained from Invitrogen Corporation. HeLa cells were cultured in Dulbecco's modified Eagle's medium containing high glucose supported by 10% fetal bovine serum (v/v), 100

dx.doi.org/10.1021/ac501499y | Anal. Chem. 2014, 86, 7071−7078

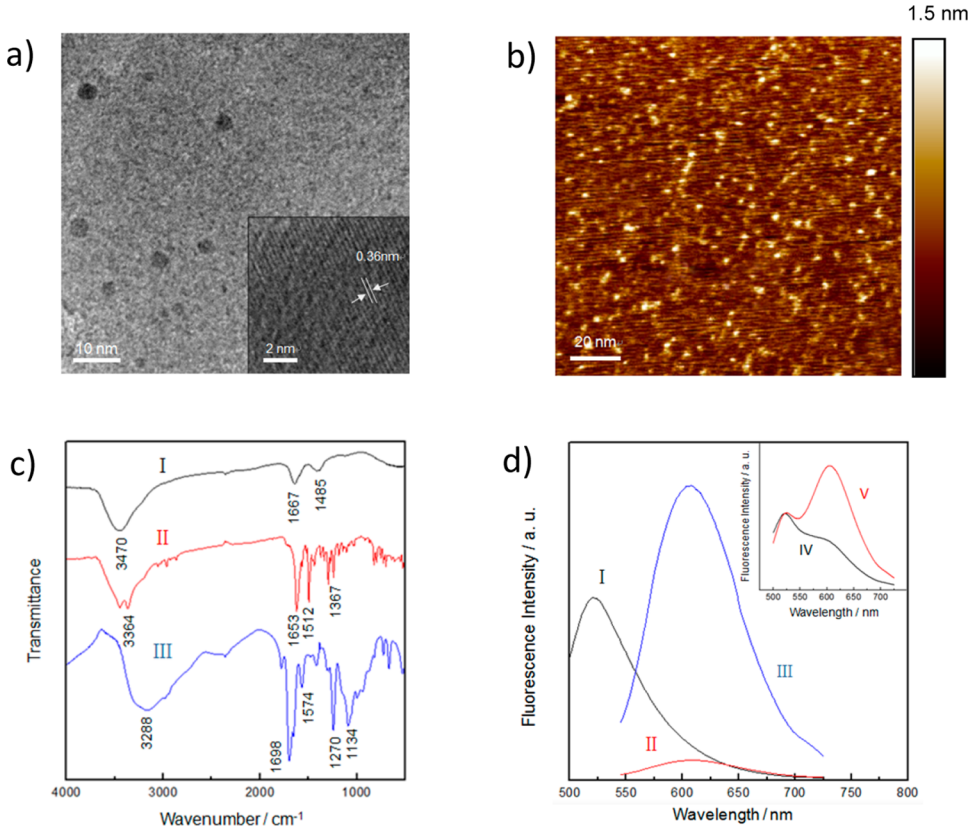

Figure 1. (a) TEM image of C-Dots and HRTEM image of typical C-Dots (inset); (b) AFM topography image of C-Dots; (c) FT-IR spectra of (I) the as-prepared C-Dots, (II) HE, and (II) CD-HE; (d) fluorescence emission spectra of (I) C-Dots, (II) HE, (III) the products of HE after being reacted with $O_2^{\bullet-}$ upon the excitation at 488 nm. Inset: Fluorescence emission spectra of (IV) CD-HE and (V) the product of CD-HE after being reacted with $O_2^{\bullet-}$ (upon the excitation at 488 nm).

μg mL^{-1} streptomycin, and 100 units mL^{-1} penicillin. HeLa cells (3×10^5 cell/mL) were then cultured onto a 96-well μL plate to a total volume of 100 μL/well in an atmosphere (5% CO_2 and 95% air) at 310 K humidified incubator for 24 h. The cytotoxicity of CD-HE was tested as follows.[43,44] First, HeLa cells were incubated in culture media with the addition of CD-HE probes at 0.001, 0.01, 0.1, 1, and 10 mg mL^{-1} for 24 and 48 h, respectively. Next, cells were washed with the culture media, and the fresh culture media containing MTT was dropped to each well followed by incubation for 4 h to allow the formation of formazan dye. Then, after DMSO was added to each well, the supernatant was removed. At last, the plate was shaken for 10 min. The cell viability was determined using the formula: cell viability (%) = (mean of absorbance value of treatment group/mean absorbance value of control group) × 100%.

Apoptosis Assay. Apoptosis assay was implemented by Annexin V-FITC Apoptosis Detection Kit. HeLa cells were incubated with CD-HE probes at 0.01, 0.1, 1 mg mL^{-1} for 24 h. After dye treatment, the cell culture medium was collected to retain floating cells and attached cells were dislodged using the EDTA-free trypsin. Floating and attached cells were combined and harvested by centrifugation. The cell pellets were suspended in 500 μL of binding buffer and incubated with 5 μL of FITC AnnexinV and 5 μL of a propidium iodide solution for 15 min in the dark. A Becton-Dickinson flow cytometer was used for the flow cytometry (FACS) measurements.

In Vivo Fluorescence Imaging. The cultured cells were plated on a Petri dish in advance 1 day before imaging studies in vitro. Next, the cells were incubated at 310 K for 1 h in 2 mL of culture media containing 2 μL of CD-HE solution. Then, the HeLa cells were washed with Hank's Balanced Salt Solution (HBSS, pH = 7.4) three times and cells were cultured in HBSS throughout the experiments. The confocal fluorescence imaging in live cells were obtained with an Olympus confocal microscope equipped with an oil immersion 60 objective. The fluorescent imaging of C-Dots was collected from a 500 to 560 nm channel, while that of HE was obtained from a 570 to 630 nm channel, by excitation at 488 nm wavelength. For the determination of the generated $O_2^{\bullet-}$ in live cells, LPS (100 μM) was added and fluorescence microscopic images were then acquired after several minutes.

RESULTS AND DISCUSSION

Characterization of C-Dots and CD-HE Probe. As a starting point of our study, the C-Dots were synthesized by the previous electrochemical method.[45] A typical TEM image (Figure 1a) shows that the as-prepared C-Dots are monodispersed with an average size of 3−5 nm. A further close observation (inset in Figure 1a) reveals that the lattice spacing of the C-Dot is consistent with the ⟨002⟩ spacing of graphitic carbon.[17] From the height view of AFM image (Figure 1b), we can see the average thickness of C-Dots is around 1−2 nm. The infrared spectrum of the C-Dots is given in Figure 1c (curve I). The band located at ∼3470 cm^{-1} corresponds to the O−H stretching mode, while the peak observed at 1485 cm^{-1} is ascribed to the C═C stretch of the polycyclic aromatic hydrocarbons. The band at around 1667 cm^{-1} indicates the existence of carbonyl groups (C═O). These data demonstrate

dx.doi.org/10.1021/ac501499y | Anal. Chem. 2014, 86, 7071−7078

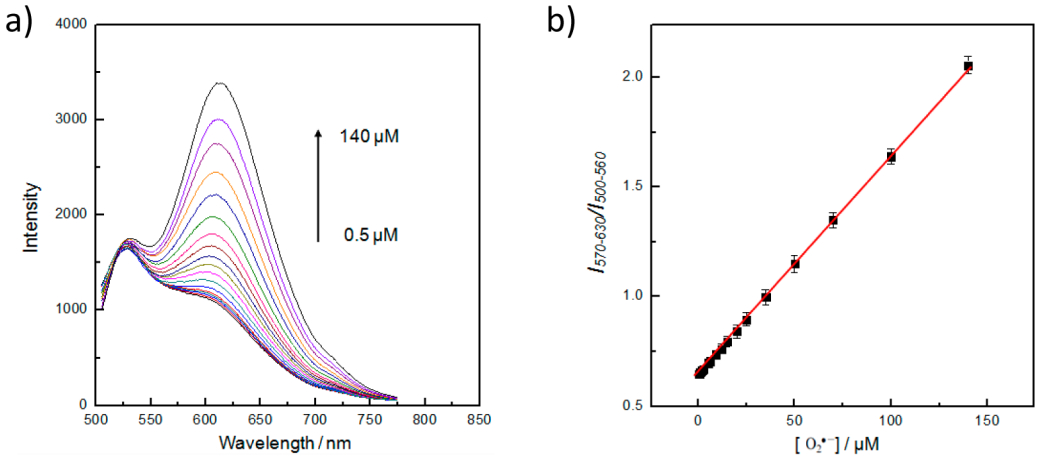

Figure 2. (a) Fluorescence emission spectra (λ_{ex} = 488 nm) of CD-HE, with the addition of different concentrations of $O_2^{\bullet-}$ (0, 0.5, 1, 1.5, 2, 2.5, 6, 9, 12, 15, 20, 25, 35, 50, 70, 100, 140 μM) and (b) plot of $I_{570-630}/I_{500-560}$ as a function of $O_2^{\bullet-}$ concentration obtained with CD-HE in PBS (pH 7.4).

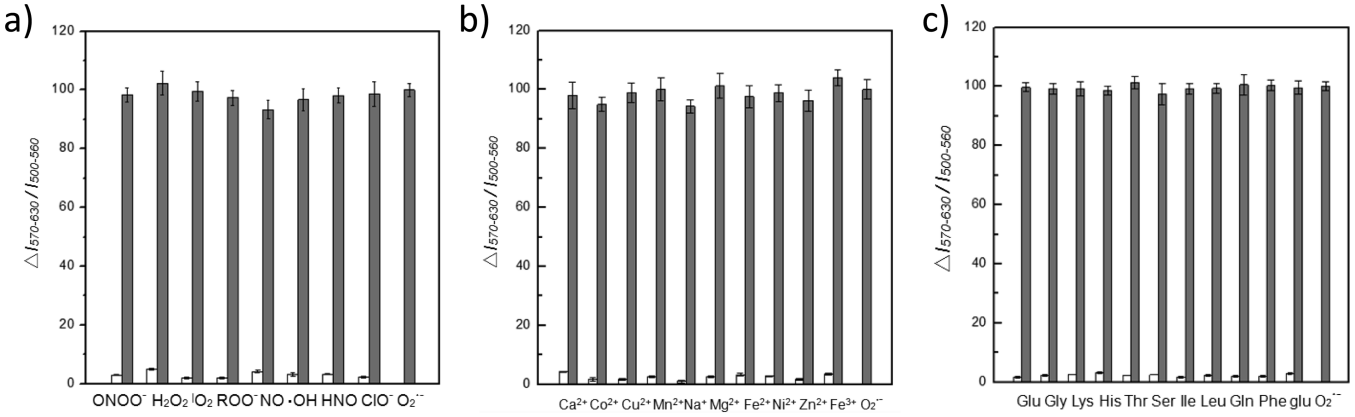

Figure 3. Selectivity and competition tests of the CD-HE probe toward (a) various ROS, (b) metal ions, and (c) amino acids and glucose. The white bars mean the addition of potential interferences. The black bars mean the subsequent addition of 10 μM $O_2^{\bullet-}$ into the fluorescent probe: (a) $ONOO^-$, H_2O_2, $^1O_2$, ROO^-, NO, $^\bullet OH$, HNO, ClO^-, 10 μM; (b) Ca^{2+}, Co^{2+}, Cu^{2+}, Mn^{2+}, Na^+, Mg^{2+}, Fe^{2+}, Ni^{2+}, Zn^{2+}, Fe^{3+}, 10 μM; (c) Glu, Gly, Lys, His, Thr, Ser, Ile, Leu, Gln, Phe, glucose, 10 μM.

that the as-synthesized C-Dots are surrounded by −COOH and −OH groups.[45] As shown in curve II (Figure 1c), the peaks observed at 3364 and 1653 cm^{-1} correspond to the stretching of N−H groups of HE. Then, C-Dots were conjugated with HE by using EDC and NHS to form an organic−inorganic fluorescent probe CD-HE. The attachment of HE onto the surface of C-Dots was also confirmed by IR spectroscopy. The bands clearly obtained in curve III at 3288 cm^{-1} (ν_{O-H}), 1698 cm^{-1} ($\nu_{C=O}$), and 1574 cm^{-1} (ν_{N-H}) suggest the successful attachment of HE onto the surface of C-Dots.

UV−vis absorption peak of C-Dots was observed at ∼250 nm, which is considered as a typical absorption of the aromatic π system. Upon the excitation at 488 nm, the C-Dots show a distinct fluorescence emission at 525 nm (curve I, Figure 1d). The fluorescence quantum yield (QY) of C-Dots was estimated to be 7.9% at the excitation wavelength of 488 nm (Figure S1, Supporting Information), using rhodamine B as a standard.[46] On the other hand, as shown in Figure 1d, HE presents almost no fluorescence by excited at 488 nm (curve II), but it emits with a peak at 610 nm (curve III). Upon the same excitation, the inorganic−organic probe CD-HE exhibits one obvious peak at 525 nm and one shoulder at 610 nm (curve IV). However, after reaction with $O_2^{\bullet-}$, as expected, two clear emission peaks of hybrid CD-HE were observed at 525 and 610 nm, respectively (curve V).

Determination of $O_2^{\bullet-}$ Based on CD-HE Probe. The working principle of this ratiometric fluorescent probe is illustrated in Scheme 1. The organic molecule HE plays double roles: one is the specific recognition element toward $O_2^{\bullet-}$; another is the response element for recognition of $O_2^{\bullet-}$ because of the increasing fluorescence intensity of HE products with the specific reaction with $O_2^{\bullet-}$. On the other hand, C-Dots serves as the reference signal element due to good stability even with the addition of $O_2^{\bullet-}$. As a proof-of-concept, responses of the developed inorganic−organic fluorescent probe toward the ratiometric determination of $O_2^{\bullet-}$ were performed, as demonstrated in Figure 2a. The ratiometric fluorescent probe CD-HE characterizes one emission peak at 525 nm and one shoulder at 610 nm, under an excitation at 488 nm. With the increasing concentration of $O_2^{\bullet-}$, the emission intensity at 610 nm attributed to HE product gradually enhanced, while the emission at 525 nm from C-Dots almost remained constant. This dual-emission ratiometric probe upon one excitation provided an inner reference for correcting the environmental errors, thus improving accuracy of the present method. As plotted in Figure 2b, the intensity ratio of two emission

dx.doi.org/10.1021/ac501499y | Anal. Chem. 2014, 86, 7071−7078

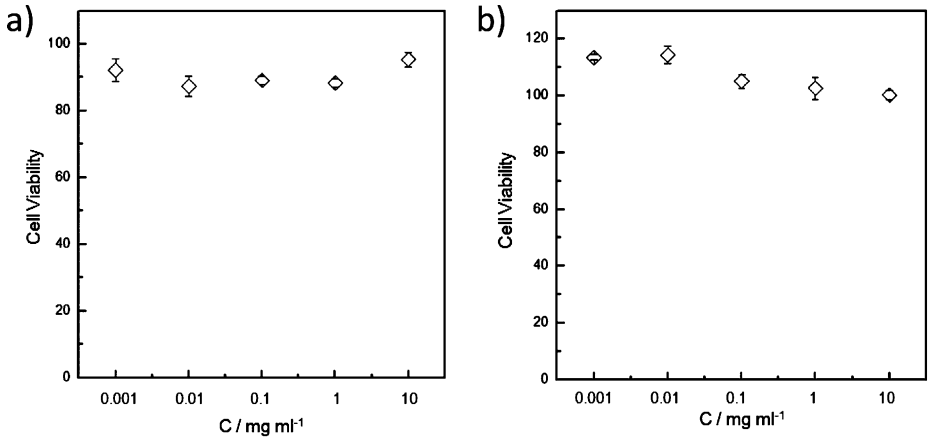

Figure 4. Cells viability (%) obtained by MTT proliferation experiments. HeLa cells were incubated with CD-HE at the concentration of 0.001, 0.01, 0.1, 1, 10 mg mL^{-1} for (a) 24 h and (b) 48 h at 310 K.

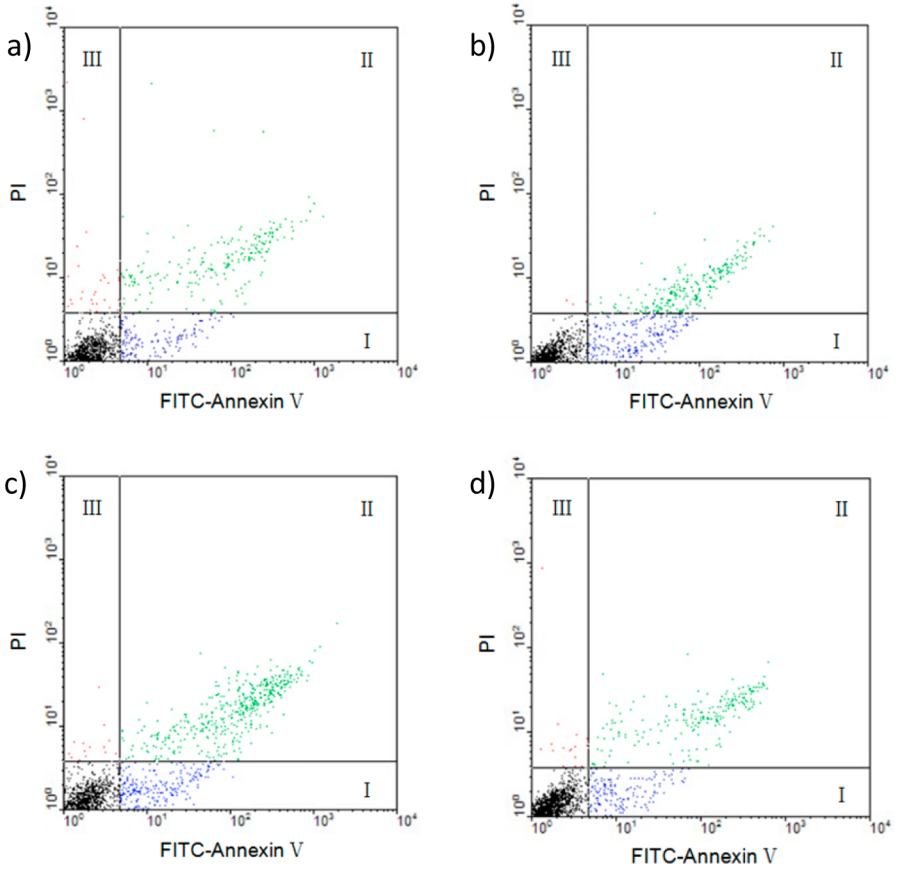

Figure 5. Apoptosis assay of HeLa cells incubated with CD-HE at concentrations of (a) 0, (b) 0.01 mg mL^{-1}, (c) 0.1 mg mL^{-1}, (d) 1 mg mL^{-1} for 24 h. Sections I, II, and III represent the regions of early apoptotic cells, late apoptotic cells, and dead cells, respectively.

channels ($I_{570-630}/I_{500-560}$) shows good linearity with the concentration of $O_2^{\bullet-}$ in the range ~5 × 10^{-7}–1.4 × 10^{-4} M. The detection limit (S/N = 3:1) was achieved to ~100 nM. Compared with those reported $O_2^{\bullet-}$ fluorescent probes,[29,30] the present inorganic–organic probe exhibited higher sensitivity and lower detection limit.

With the applications to live cells, not only sensitivity but selectivity is also a challenging work to the analytical method. Next, the selectivity test was performed by monitoring the changes of emission intensity ratio ($\Delta I_{570-630}/I_{500-560}$) with the addition of potential interferences, compared with that from $O_2^{\bullet-}$. Reactive oxygen species (ROS) including $^{\bullet}OH$, H_2O_2, $^1O_2$, $ONOO^-$, and so on, as well as metal ions such as Ca^{2+}, Co^{2+}, Cu^{2+}, etc., and amino acids that may coexist in the live cells were examined under the same conditions. As summarized in Figure 3a, negligible interferences (<5%) were observed for other ROS. Moreover, the effects on the signal for $O_2^{\bullet-}$ sensing of the potential ROS interferences were neglected. Meanwhile, no obvious responses were observed for metal ions (Figure 3b), amino acids and glucose (Figure 3c). The metal ions, amino acids, and glucose also showed little effects on the reponses of fluorescent probes. The experimental results indicated that the

dx.doi.org/10.1021/ac501499y | Anal. Chem. 2014, 86, 7071–7078

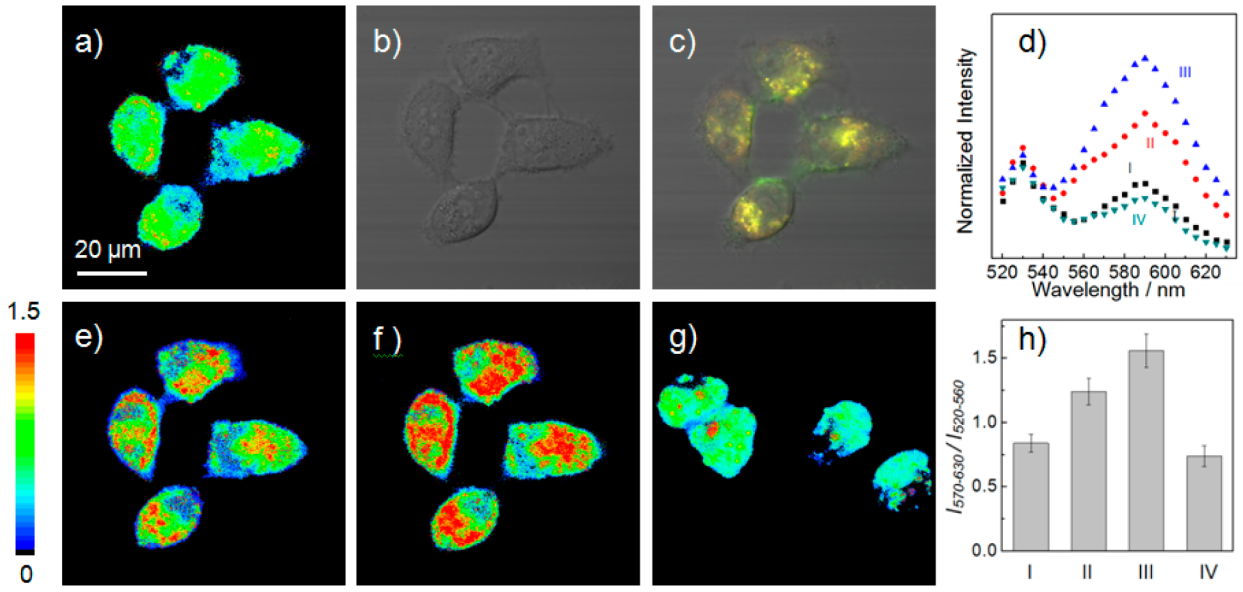

Figure 6. (a) Pseudocolored ratiometric image ($I_{570-630}/I_{500-560}$) of HeLa cells after incubation with CD-HE probes, (b) bright-field image, and (C) overlay of confocal fluorescence image and the bright-field image of HeLa cells containing CD-HE probes excited by 488 nm. (D) Intracellular fluorescence emission scan (I) before addition of LPS, (II) after induced by 8 μg mL^{-1} LPS for 40 min, (III) 60 min, and (IV) pretreated with 10 μg mL^{-1} GSH for 30 min and then induced by LPS for 60 min. (E, F) Pseudocolored ratiometric images of HeLa cells containing CD-HE probes after induced by LPS for 40 and 60 min, respectively. (G) The ratiometric image pretreated with 10 μg mL^{-1} GSH for 30 min and then stimulated by LPS for 60 min. (H) A bar graph showing the integrated fluorescence intensity from 570 to 630 nm over the integrated intensity from 500 to 560 nm. Values are the mean ratios obtained from the intensities from five randomly selected fields. The error bars mean standard error measurements (SEM). (I) before addition of LPS, (II) after induction by LPS for 40 min and (III) 60 min, and (IV) in the presence of GSH before induction by LPS for 60 min.

developed hybrid fluorescence probe exhibited good selectivity for $O_2^{\bullet-}$ over other ROS, metal ions, amino acids, and so on. Actually, the reaction mechanism between hydroethidine (HE) and superoxide ($O_2^{\bullet-}$) is very complicated. The red fluorescent product of HE reaction with $O_2^{\bullet-}$ has long been assumed to be the two-electron oxidation product ethidium (E^+). However, recently, E^+, 2-hydroxyethidium (2-OH-E^+), and even the dimeric products have been reported in extracts from cells incubated with HE.[47] Anyway, the reaction products between HE and $O_2^{\bullet-}$ can emit at 590−620 nm by the excitation at 500−530 nm. The other ROS including H_2O_2, $^{\bullet}OH$, $ONOO^-$, and so on can rapidly react with HE but not forming these characteristic products with emission at 590−620 nm.[47] Clearly, additional studies are needed before we can understand the reason why HE is specific to $O_2^{\bullet-}$.

In addition, the C-Dot-based probe was also independent of solution pH in the broad pH range from 6.0 to 9.0. (Figure S2 in the Supporting Information), which fulfills the requirement for monitoring of $O_2^{\bullet-}$ in the biological system. To test the stability, the inorganic−organic probe was consecutively irradiated at 488 nm. No significant change (<10%) was observed under continuous excitation for ∼2 h (Figure S3, Supporting Information).

Cytotoxicity. For a further biological application point of view, MTT assays were first employed to evaluate cytotoxicity of the inorganic−organic probe. As shown in Figure 4, the viability of HeLa cells still maintained >90% after incubation for 24 h (a) and 48 h (b), with the fluorescent probe up to 10 mg mL^{-1}, which is 100 times higher than that used in cell experiments (0.1 mg mL^{-1}). Thus, the results suggest that the probe can be considered to be low toxicity for live cells.

Apoptosis assay of HeLa cells incubated with CD-HE probe was further taken to judge the biocompatibility of this fluorescence probe by flow cytometry (FACS) measurements. The live cells were dyed by FITC-annexin V and propidium iodide to label the apoptosis cells and necrotic cells, respectively, for FACS measurements. Sections I, II, and III in Figure 5 demonstrate the regions of early apoptotic cells, late apoptotic cells, and dead cells, respectively. From the results, we can clearly see that there are no prominent difference between blank cells (a) and the cells treated with the fluorescent probes with different concentrations (b−d), suggesting that the CD-HE probe shows good biocompatibility.

Intracellular Bioimaging and Biosensing of $O_2^{\bullet-}$. As described above, the as-prepared ratiometric fluorescent probe CD-HE, which exhibits high sensitivity, selectivity, and accuracy, together with long-term stability and good biocompatibility, established a reliable and durable approach for intracellular bioimaging and biosening of $O_2^{\bullet-}$. For this purpose, HeLa cells were first uptook by the CD-HE probe for ∼1 h, then washed with HBSS three times. Followed by that, the CD-HE fluorescent probe in HeLa cells was tracked by confocal microscopy. Figure 6 shows a pseudocolored ratiometric image ($I_{570-630}/I_{500-560}$) of HeLa cells with CD-HE probes (Figure 6a), bright-field image (Figure 6b) and the overlay fluorescence image and bright-field image (Figure 6c) of the probes in live cells. From the overlay image, we can see that the probe had good cell-permeability and transferred into live cells within 30 min. The present probe entered the cell membrane and is located in cytoplasm, as demonstrated in Figure 6c. The observation was further evident by the nuclear staining experiment, which was performed using Hoechst 33342 as the nucleus stain. It was found that the CD-HE

dx.doi.org/10.1021/ac501499y | Anal. Chem. 2014, 86, 7071−7078

probes were obviously located in cytoplasm and near the cell nucleus (Figure S4 in the Supporting Information). The fluorescence scan in live cells also demonstrated that the ratiometric probes entered into live cells and maintained the dual-emission in a cellular environment, as shown in Figure 6d. As a matter of fact, the ratio images were collected from two separated channels (Figure S4 in the Supporting Information, 500−560 nm, I_{green}, and 570−630 nm, I_{red}). From Figure 6d, the average emission ratio I_{red}/I_{green} was estimated to 0.78 ± 0.07, indicating a low levels of available $O_2^{\bullet-}$ in the normal conditions. Then, the I_{red}/I_{green} ratio gradually increased to 1.24 ± 0.10 and 1.53 ± 0.13 when the cells were induced with LPS, a stimulator for production of ROS, for 40 and 60 min, respectively. The false color obviously turned from green to red, as demonstrated in Figure 6e,f. From the fluorescence images of separated channels as shown in Figure S5 in the Supporting Information, it is clear that only the fluorescence of HE increased with the reaction of $O_2^{\bullet-}$, while negligible changes were obtained for C-Dots channel. In order to identify the fluorescence enhancement of the HE channel ascribed to the production of $O_2^{\bullet-}$, cells were pretreated with a $O_2^{\bullet-}$ scavenger, GSH, and then stimulated by LPS. As shown in Figure 6g, the fluorescence ratio turned back to 0.74 ± 0.08, and false color also changed in green. This observation suggests that the observed changes of fluorescence ratios after induced by LPS were attributed to the $O_2^{\bullet-}$ release in live cells. These fundmental experiments in live cells implied that the developed dual-emission CD-HE probe provided a reliable approach for further biology research.

CONCLUSIONS

A C-Dot-based fluorescence biosensor for ratiometric monitoring of $O_2^{\bullet-}$ has been developed for intracellular bioimaging and biosensing, in which C-Dot is employed as a reference signal and HE plays the role as both response signal and specific recognition element. The inorganic−organic fluorescent sensor demonstrates high sensitivity, selectivity, and accuracy, which fulfills the requirements for determination of $O_2^{\bullet-}$ in live cells. Furthermore, the C-Dot-based probe is pH-independent in the range of 6.0−9.0 and shows long-term stability against light illumination, low cytotoxicity, and high biocompatibility. Thus, the developed fluorescent biosensor for $O_2^{\bullet-}$ with great analytical performance and remarkable characteristic of C-Dots has been successfully contributed to ratiometric imaging and real-time biosensing the changes of $O_2^{\bullet-}$ level upon oxidative stress. The present study has opened up a new way to determination of $O_2^{\bullet-}$ in living systems. This method can be extended to design and construct the ratiometric biosensors for other ROS and related species, for further understanding of their critical roles in the biological and pathological events.

ASSOCIATED CONTENT

Supporting Information

Quantum yield calculations, pH stability, stability upon light illumination, nuclear staining experiments, and confocal fluorescence images of probe with separated channels in live cells. This material is available free of charge via the Internet at http://pubs.acs.org.

AUTHOR INFORMATION

Corresponding Author

*E-mail: ytian@chem.ecnu.edu.cn. Phone: +86-21-62237105. Fax: +86-21-62237105.

Notes

The authors declare no competing financial interest.

ACKNOWLEDGMENTS

This work was financially supported by the NSFC (Grant 21175098) and the National Natural Science Fund for Distinguished Young Scholars (Grant 21325521).

REFERENCES

(1) Bergamini, C.; Gambetti, S.; Dondi, A.; Cervellati, C. *Curr. Pharm. Des.* **2004**, *10*, 1611−1626.
(2) Thannickal, V.; Fanburg, B. *Am. J. Physiol. Lung Cell. Mol. Physiol.* **2000**, *279*, L1005−L1028.
(3) Sheng, Y. W.; Abreu, I.; Cabelli, D. *Chem. Rev.* **2014**, *114*, 3854−3918.
(4) Liou, G. Y.; Storz, P. *Free Radiat. Res.* **2010**, *44*, 479−496.
(5) Fridovich, I. *Annu. Rev. Biochem.* **1995**, *64*, 97−112.
(6) Gáspár, S. Detection of Superoxide and Hydrogen Peroxide from Living Cells Using Electrochemical Sensors. In *Oxidative Stress: Diagnostics, Prevention, and Therapy*; ACS Symposium Series, Vol. *1083*; American Chemical Society: Washington, DC, 2011; pp 289−309.
(7) Tachikawa, T.; Wang, N.; Yamashita, S.; Cui, S.-C.; Majima, T. *Angew. Chem., Int. Ed.* **2010**, *49*, 8593−8597.
(8) Naito, K.; Tachikawa, T.; Fujitsuka, M.; Majima, T. *J. Am. Chem. Soc.* **2009**, *131*, 934−936.
(9) Li, N.; Wang, H.; Xue, M.; Chang, C.; Chen, Z.; Zhuo, L.; Tang, B. *Chem. Commun.* **2012**, *48*, 2507−2509.
(10) Gao, J.; Xu, K.; Tang, B.; Yin, L.; Yang, G.; An, L. *FEBS J.* **2007**, *274*, 1725−1733.
(11) Deng, Z.; Rui, Q.; Yin, X.; Liu, H.; Tian, Y. *Anal. Chem.* **2008**, *80*, 5839−5846.
(12) Luo, Y.; Liu, H.; Rui, Q.; Tian, Y. *Anal. Chem.* **2009**, *81*, 3035−3041.
(13) Zhu, A.; Luo, Y.; Tian, Y. *Anal. Chem.* **2009**, *81*, 7243−7247.
(14) Li, X.; Liu, Y.; Zhu, A.; Luo, Y.; Deng, Z.; Tian, Y. *Anal. Chem.* **2010**, *82*, 6512−6518.
(15) Shao, X.; Gu, H.; Wang, Zhen.; Chai, X.; Tian, Y.; Shi, G. *Anal. Chem.* **2013**, *85*, 418−425.
(16) Zhu, A.; Qu, Q.; Shao, X. L.; Kong, B.; Tian, Y. *Angew. Chem., Int. Ed.* **2012**, *51*, 7185−7189.
(17) Kong, B.; Zhu, A.; Ding, C.; Zhao, X.; Li, B.; Tian, Y. *Adv. Mater.* **2012**, *24*, 5844−5848.
(18) Zhuang, M.; Ding, C.; Zhu, A.; Tian, Y. *Anal. Chem.* **2014**, *86*, 1829−1836.
(19) Zhu, A.; Ding, C.; Yang, T. *Sci. Rep.* **2013**, *3*, 2933.
(20) Zhang, W.; Li, P.; Yang, F.; Hu, X.; Sun, C.; Zhang, W.; Chen, D.; Tang, B. *J. Am. Chem. Soc.* **2013**, *135*, 14956−14959.
(21) Li, P.; Zhang, W.; Li, K.; Liu, X.; Xiao, H.; Zhang, W.; Tang, B. *Anal. Chem.* **2013**, *85*, 9877−9881.
(22) Li, H.; Li, Q.; Wang, X.; Xu, K.; Chen, Z.; Gong, X.; Liu, X.; Tong, L.; Tang, B. *Anal. Chem.* **2009**, *81*, 2193−2198.
(23) Chen, X. Q.; Tian, X. Z.; Shin, I.; Yoon, J. *Chem. Soc. Rev.* **2011**, *40*, 4783−4804.
(24) Murale, D.; Kim, H.; Choi, W. S.; Churchill, D. *Org. Lett.* **2013**, *15*, 3946−3949.
(25) Wang, X.; Sun, J.; Zhang, W.; Ma, X.; Lv, J.; Tang, B. *Chem. Sci.* **2013**, *4*, 2551−2556.
(26) Li, P.; Fan, N.; Li, K.; Tang, B. *Chem. Commun.* **2012**, *48*, 2077−2079.
(27) Tian, J.; Chen, H.; Zhuo, L.; Xie, Y.; Li, N.; Tang, B. *Chem.—Eur. J.* **2011**, *17*, 6626−6634.
(28) Sun, Y.; Zhou, B.; Lin, Y.; Wang, W.; Fernando, K. A. S.; Pathak, P.; Meziani, M. J.; Harruff, B. A.; Wang, X.; Wang, H.; Luo, P.; Yang, H.; Kose, M. E.; Chen, B.; Veca, L. M.; Xie, S. *J. Am. Chem. Soc.* **2006**, *128*, 7756−7757.

(29) Wang, X.; Cao, L.; Yang, S.; Lu, F.; Meziani, M.; Tian, L.; Sun, K.; Bloodgood, A. M.; Sun, Y. *Angew. Chem., Int. Ed.* **2010**, *49*, 5310−5314.
(30) Yang, S. T.; Wang, X.; Wang, H.; Lu, F.; Luo, P.; Cao, L.; Meziani, M. J.; Liu, J.; Liu, Y.; Chen, M.; Huang, Y.; Sun, Y. *J. Phys. Chem. C* **2009**, *113*, 18110−18114.
(31) Zheng, L.; Chi, Y.; Dong, Y.; Lin, Y.; Wang, B. *J. Am. Chem. Soc.* **2009**, *131*, 4564−4565.
(32) Zhao, H. T.; Kalivendi, S.; Joseph, J.; Zhang, H.; Kalyanaraman, B. *Free Radical Biol. Med.* **2002**, *33*, 425−431.
(33) Peshavariya, H. M.; Dusting, G. J.; Selemidis, S. *Free Radiat. Res.* **2007**, *41*, 699−712.
(34) Chen, J.; Rogers, S.; Kavdia, M. *Ann. Biomed. Eng.* **2013**, *41*, 327−337.
(35) Georgiou, C.; Papapostolou, I.; Patsoukis, N.; Tsegenidis, T.; Sideris, T. *Anal. Biochem.* **2005**, *347*, 144−151.
(36) Zielonka, J.; Hardy, M.; Kalyanaraman, B. *Free Radical Biol. Med.* **2009**, *46*, 329−338.
(37) Robinson, K.; Janes, M.; Pehar, M.; Monette, J.; Ross, M.; Hagen, T.; Murphy, M.; Beckman, J. *Proc. Natl. Acad. Sci. U.S.A.* **2006**, *103*, 15038−15043.
(38) Back, P.; Matthijssens, F.; Vanfleteren, J.; Braeckman, B. *Anal. Biochem.* **2012**, *423*, 147−151.
(39) Skatchkov, M.; Sperling, D.; Hink, U.; Anggard, E.; Munzel, T. *Biochem. Biophys. Res. Commun.* **1998**, *248*, 382−386.
(40) Zhang, L.; Tang, B.; Ding, Y. *J. Agric. Food Chem.* **2005**, *53*, 549−553.
(41) Kishioka, S.; Takekawa, T.; Yamada, A. *Anal. Sci.* **2004**, *20*, 1465−1466.
(42) Kutala, V. K.; Parinandi, N.; Zweier, J.; Kuppusamy, P. *Arch. Biochem. Biophys.* **2004**, *424*, 81−88.
(43) Vergun, O.; Sobolevsky, A.; Yelshansky, M.; Keelan, J.; Khodorov, B.; Duchen, M. *J. Physiol.* **2001**, *531*, 147−163.
(44) Patra, C. R.; Kim, J. H.; Pramanik, K.; d'Uscio, L. V.; Patra, S.; Pal, K.; Ramchandran, R.; Strano, M. S.; Mukhopadhyay, D. *Nano Lett.* **2011**, *11*, 4932−4938.
(45) Li, H.; He, X.; Kang, Z.; Huang, H.; Liu, Y.; Liu, J.; Lian, S.; Tsang, C. H. A.; Yang, X.; Lee, S. T. *Angew. Chem., Int. Ed.* **2010**, *49*, 4430−4434.
(46) Zhou, J.; Booker, C.; Li, R.; Zhou, X.; Sham, T.-K.; Sun, X.; Ding, Z. *J. Am. Chem. Soc.* **2007**, *129*, 744−745.
(47) Zielonka, J.; Hardy, M.; Kalyanaraman, B. *Free Radical Biol. Med.* **2009**, *46*, 329−338.